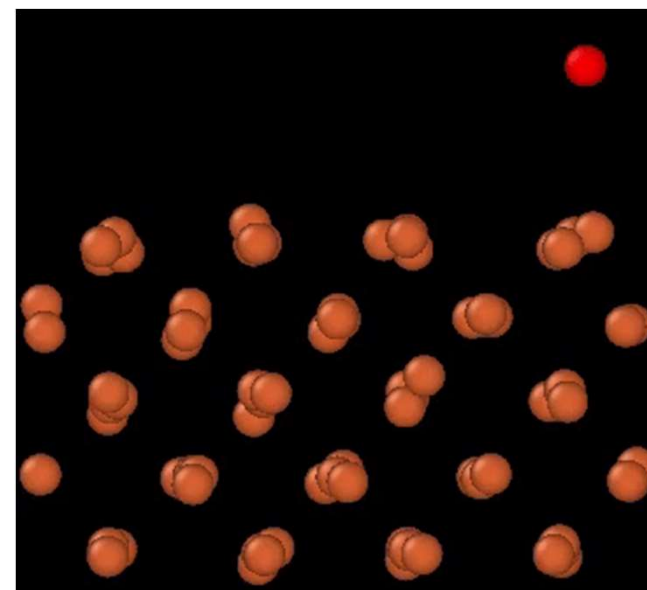


Quantum and isotope effects of hydrogen diffusivity and solubility in bcc metals

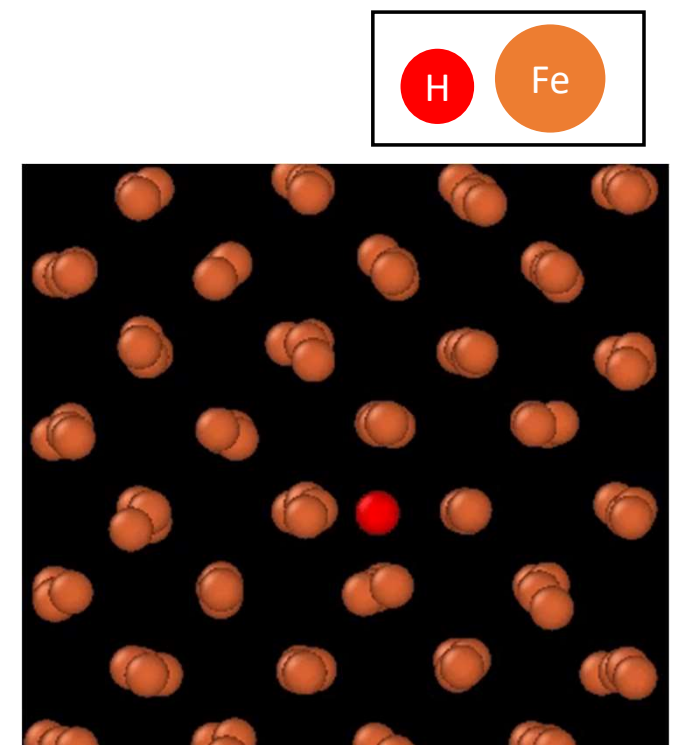
- Application of machine learning potential and path integral molecular dynamics

Hyukjoon Kwon, Takuji Oda*

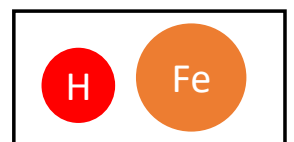
Seoul National University, South Korea.



Solution



Diffusion



1. Introduction

1.1 Hydrogen diffusion, solution, permeation in fusion reactors

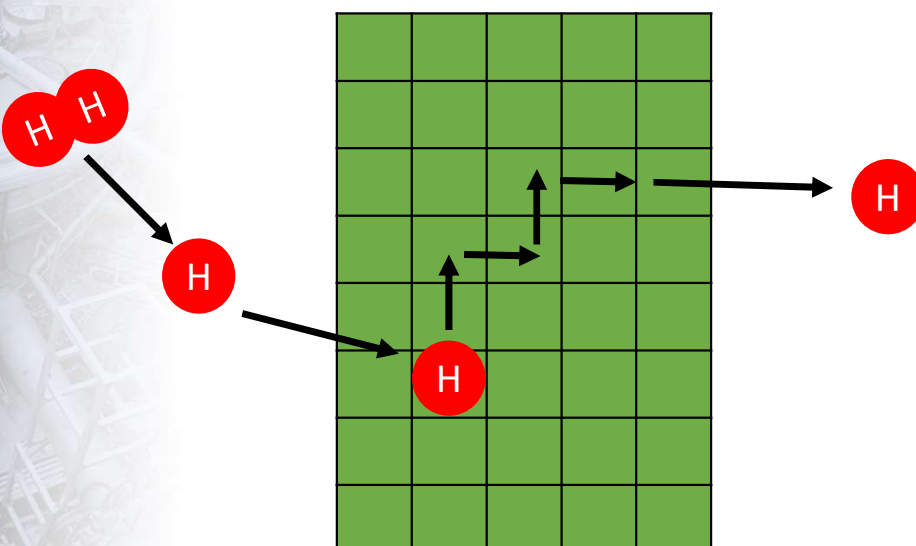


Fig1. Hydrogen permeation through lattice

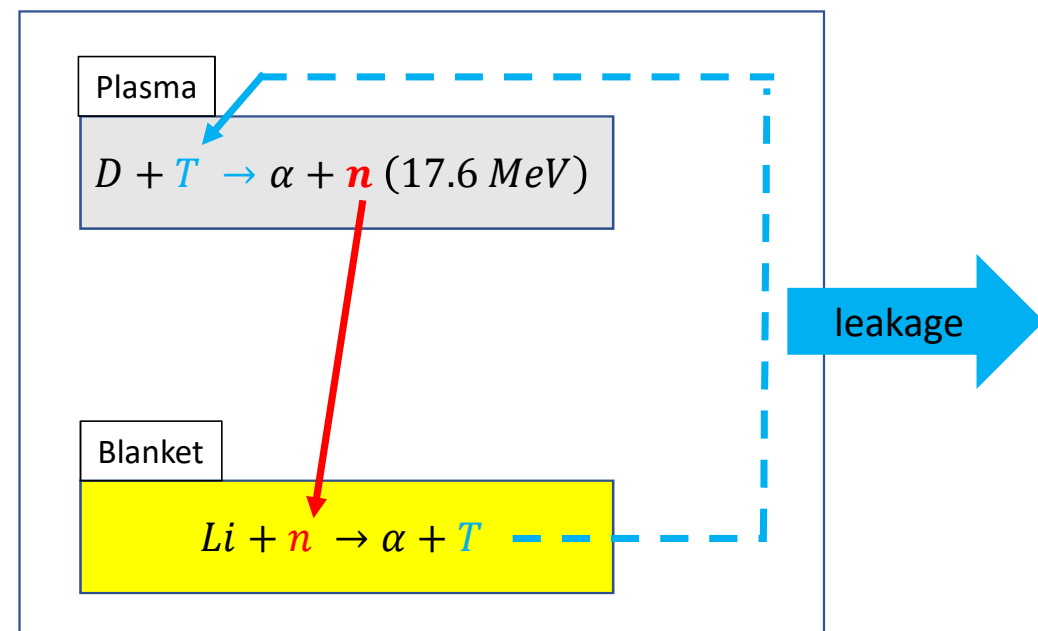


Fig2. Tritium recycling system

1. Introduction

1.2. Objective

Preceding research

Experiments:
highly affected by trapping & surface effects

Molecular Dynamics:
Ab-initio force field is required, but it's
computationally demanding

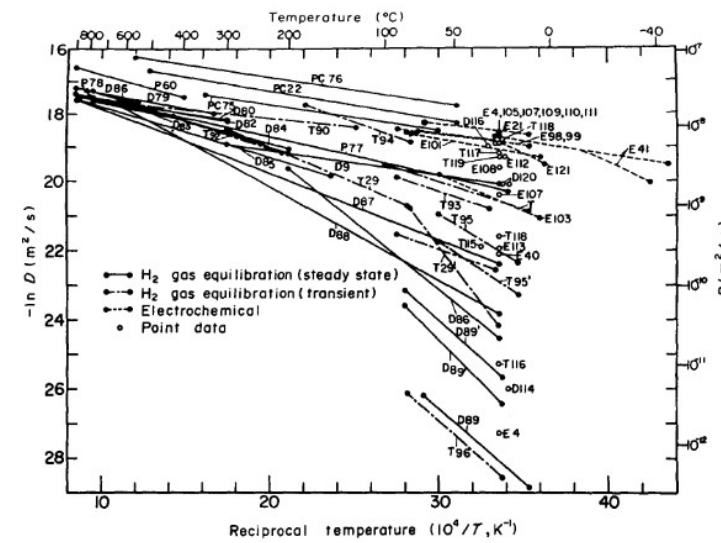


Fig3. H diffusivity in bcc Fe (experiments)
Acta Metall. 31, 961–984 (1983)

∴ Machine learning potential was generated for substituting Ab-initio calculations.
Thus, Hydrogen diffusivity and solubility in bcc Fe and W were estimated by MD simulations.

1. Machine learning interatomic potential (1/4)

■ Machine learning potential: Moment tensor potential (MTP)

- It was invented by A. V. Shapeev (2016).
- It can be trained to **imitate** a target force field (DFT-PBE) with a set of polynomials

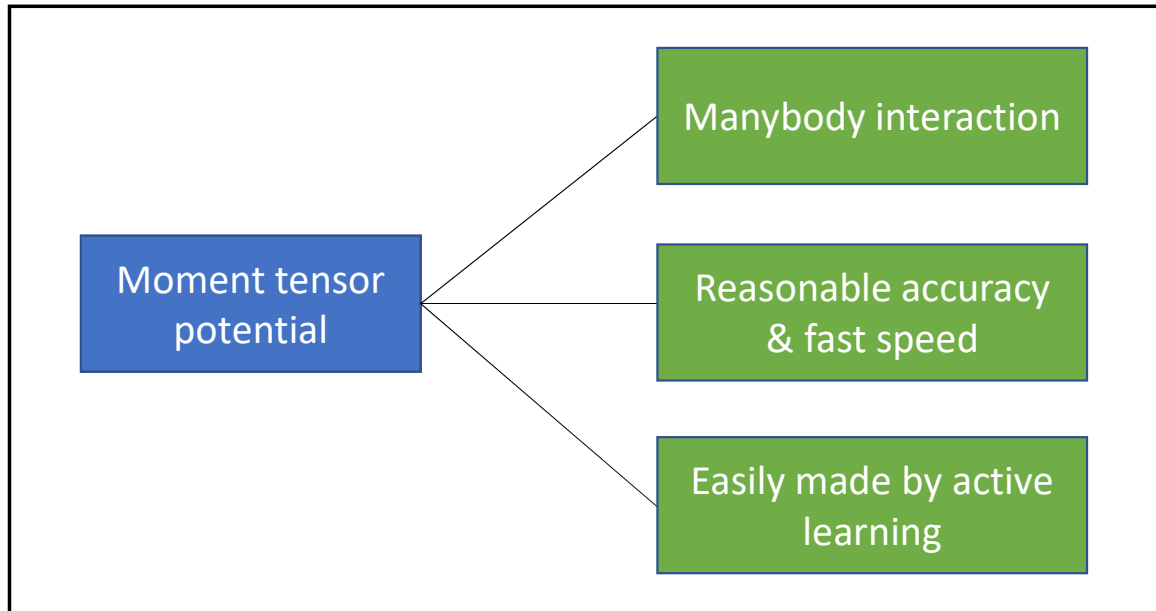
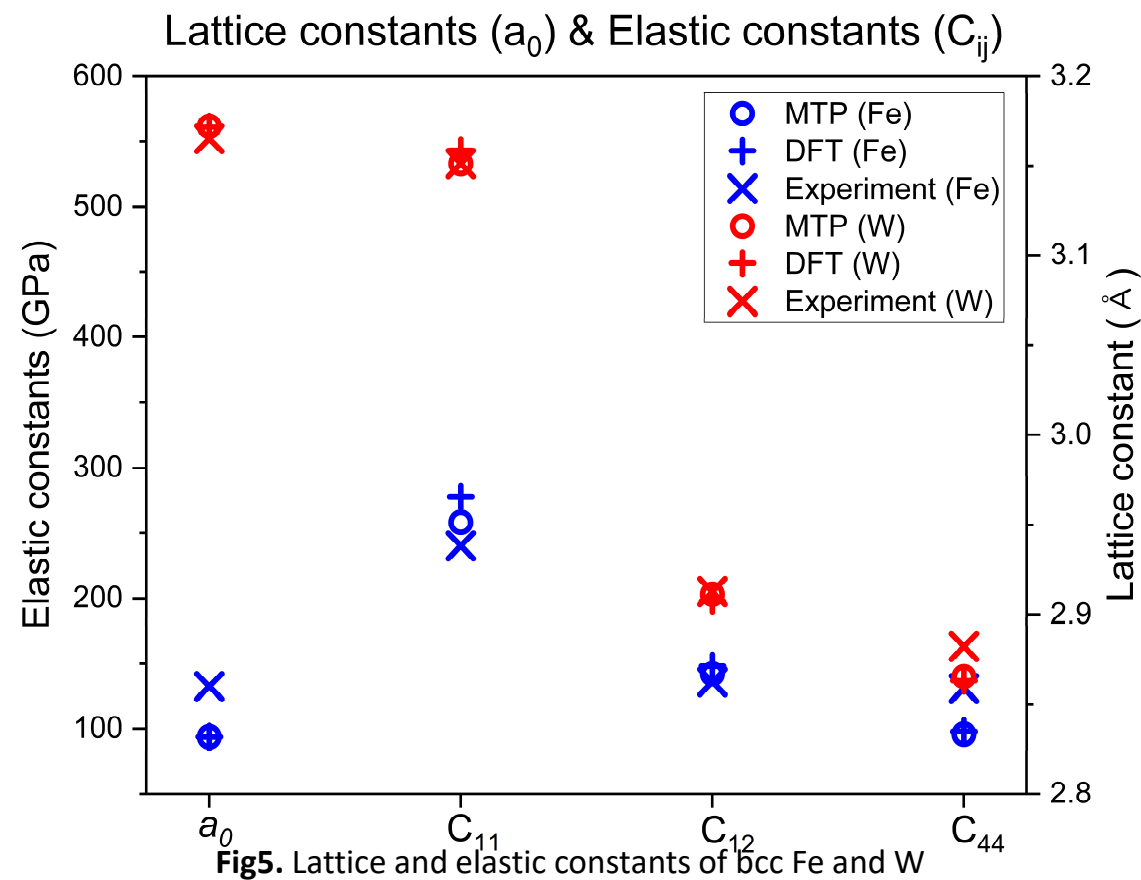


Fig4. Advantages of moment tensor potential (MTP)

1. Machine learning interatomic potential (2/4)



Lattice constant: (W) Basinski, Z. S. Series A, Mathematical and Physical Sciences, Volume 229, Issue 1179, pp. 459-467 (1955), (Fe) phys. stat. sol. 8, 2253 (1963)
Elastic constants: (W) J. Appl. Phys. 100, 113530 (2006), (Fe) F. H. Featherston and J. R. Neighbours, Phys. Rev. 130, 1324 (1963)

1. Machine learning interatomic potential (4/4)

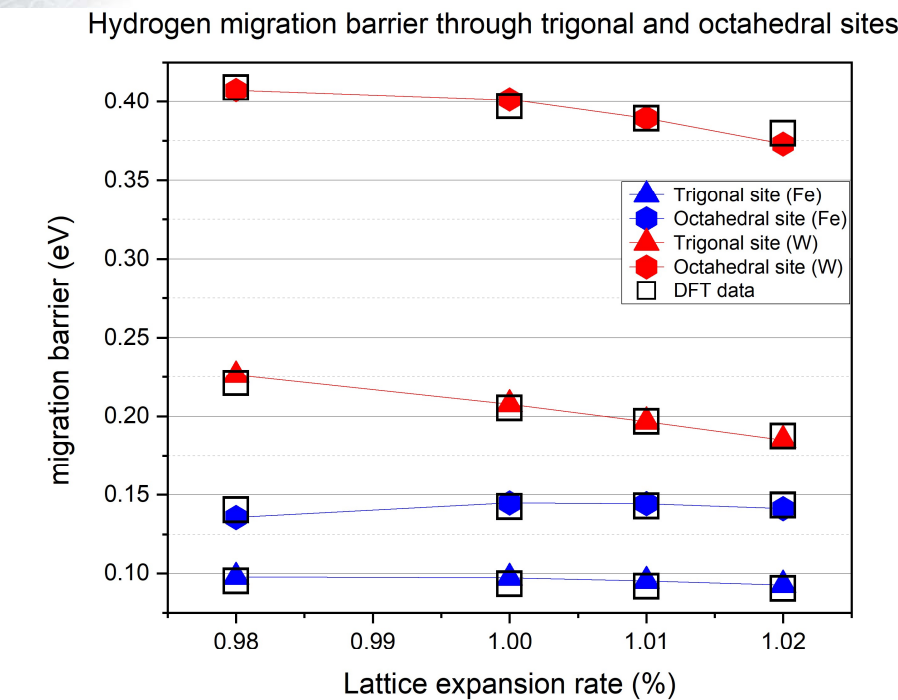


Fig6. Hydrogen Migration barrier of Trigonal and octahedral sites

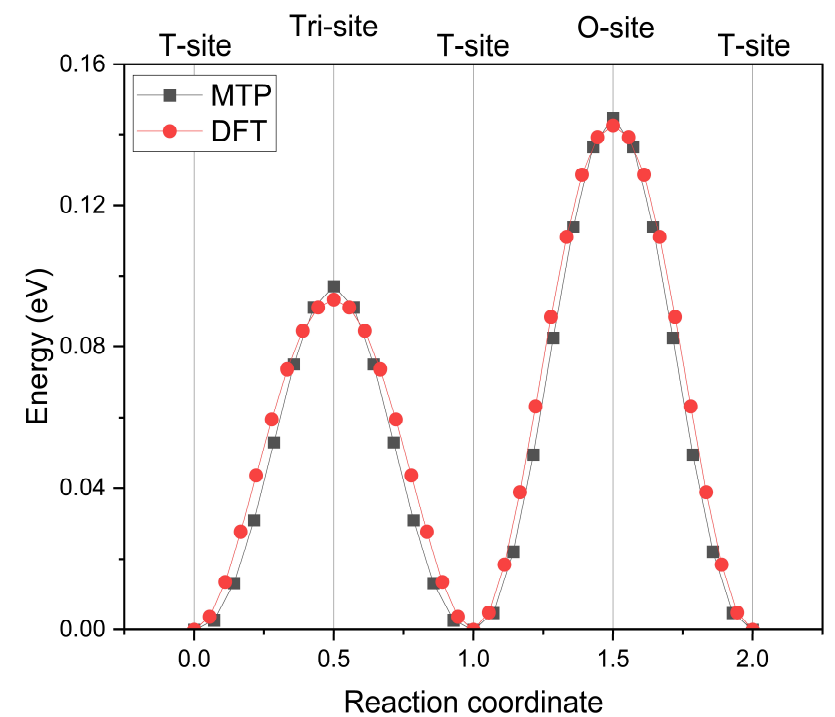


Fig7. Minimum energy path of H migration in bcc Fe (by NEB)

3. Hydrogen diffusivity in W

3.1. Outline

Diffusivity

Nuclear quantum effects
of H diffusivity

Zero point energy effects
& Quantum tunneling

Isotope effects

Diffusivity ratio $\left(\frac{D_H}{D_D}, \frac{D_H}{D_T}\right)$

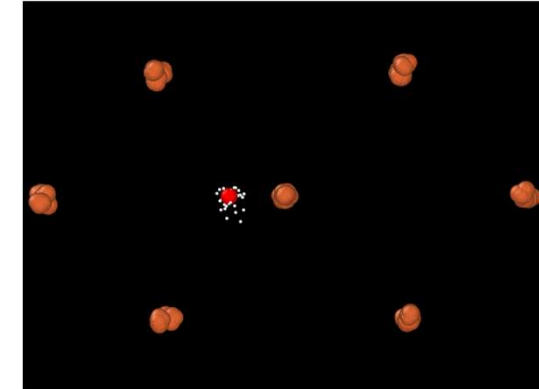


Fig8. Ring polymer molecular dynamics (RPMD)

3. Hydrogen diffusivity in W

3.2. Nuclear quantum effects

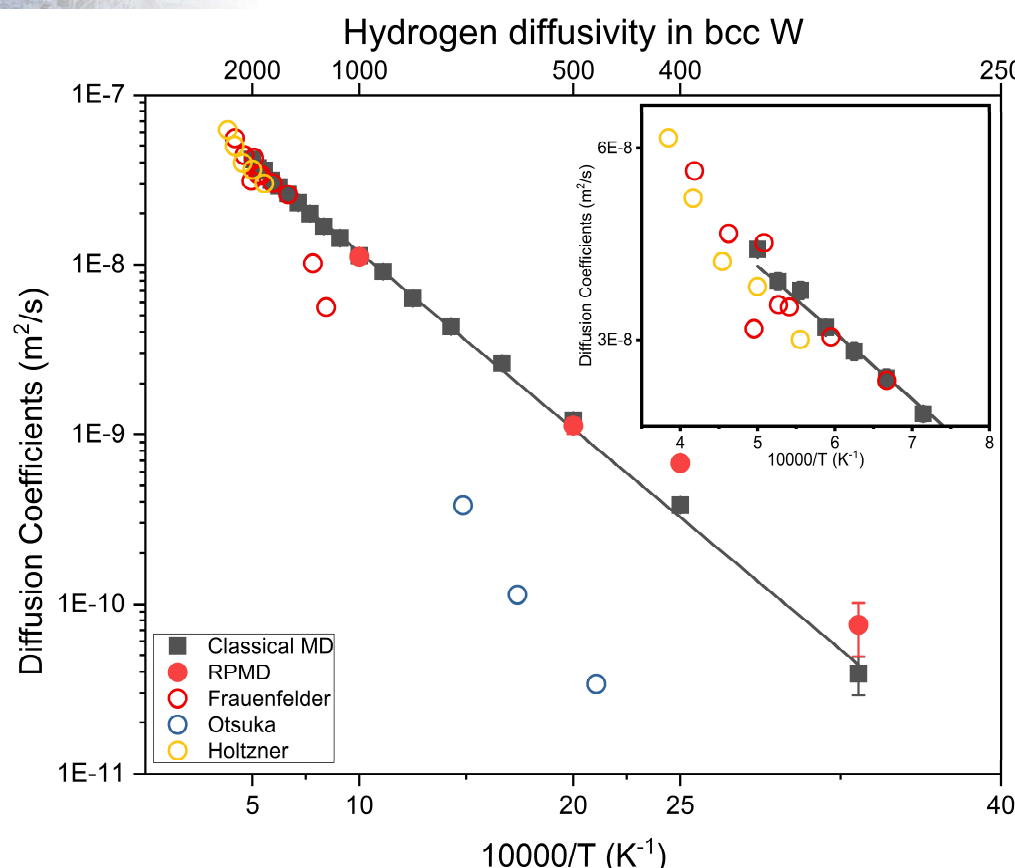


Fig9. Hydrogen diffusivity in bcc W

Notes

- Under 1500 K, experimental data seems unreliable because hydrogen diffusion is strongly limited by trapping mechanisms.
- Nuclear quantum effects could start to be visible below 400 K, although the magnitude is not large even at 300 K

R. Frauenfelder, J. Vac. Sci. Technol. 6 (1969) 388.
 Otsuka, T., Hoshihira, T. & Tanabe, Phys. Scr. TT138, (2009).
 Holzner, G., Schwarz-Selinger, Phys. Scr. 2020, (2020). 8

3. Hydrogen diffusivity in W

3.2. Nuclear quantum effect

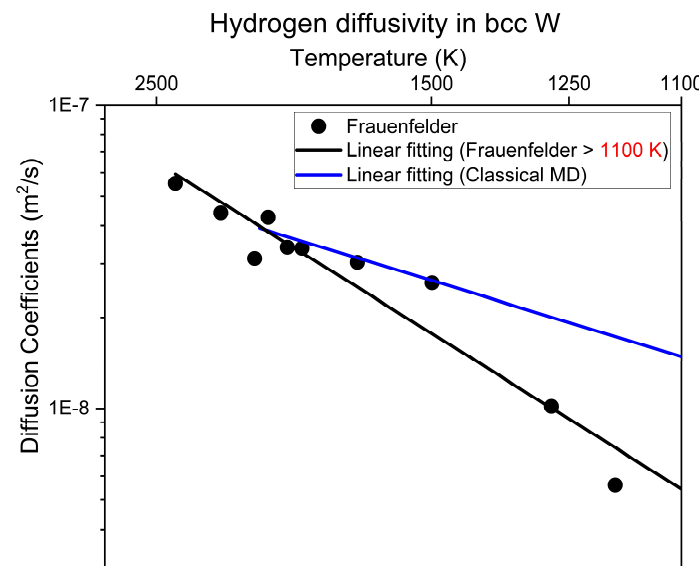


Fig10. Linear fitting of Frauenfelder's data above 1100 K

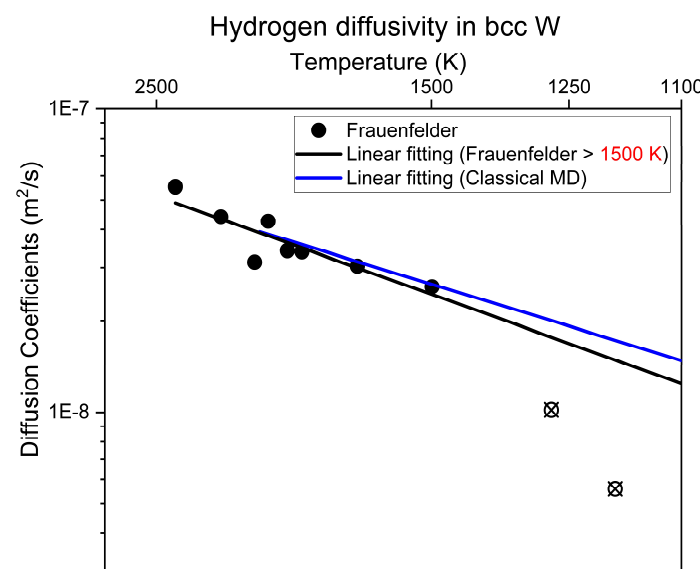


Fig11. Linear fitting of Frauenfelder's data above 1500 K

Arrhenius equation	Activation energy (eV)	Pre-exponential factor ($10^{-7} m^2/s$)
Frauenfelder (> 1100 K)	0.42 ± 0.04	4.56
Frauenfelder (> 1500 K)	0.24 ± 0.05	1.58
Holzner	0.28 ± 0.06	2.06
Classical MD	0.20 ± 0.002	1.24

Table 1. Arrhenius equation of H diffusivity in bcc W

3. Hydrogen diffusivity in W

3.3. Isotope effects above 500 K

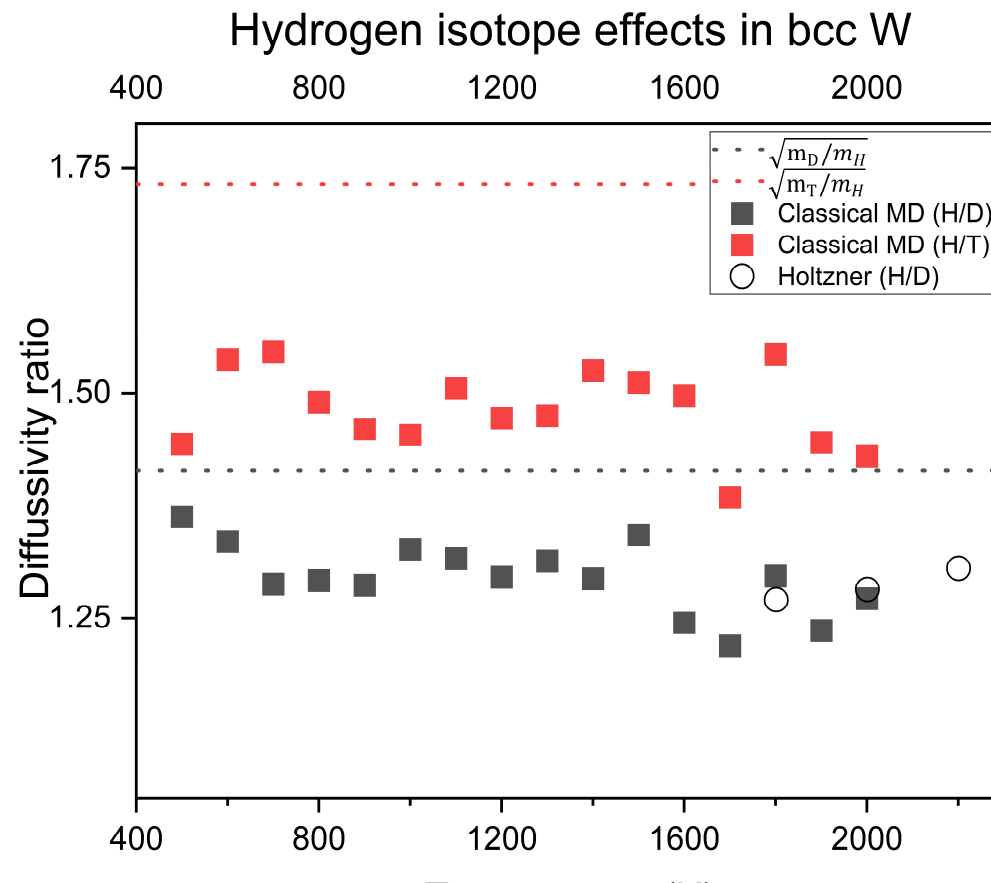


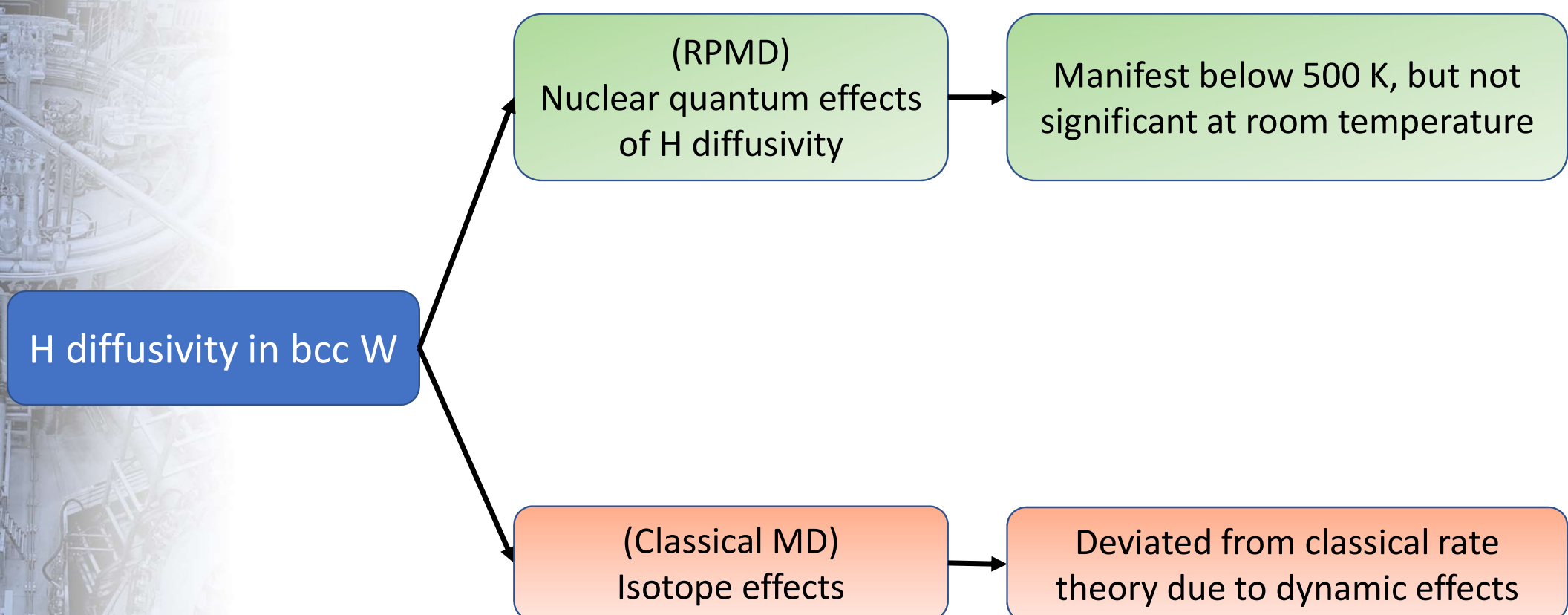
Fig12. Hydrogen isotope effects in bcc W

$$D_H/D_D < \sqrt{m_D/m_H}$$

$$D_H/D_T < \sqrt{m_T/m_H}$$

3. Hydrogen diffusivity in W

3.4. Summary



4. Hydrogen solubility in bcc Fe

4.1. Outline (1/4)

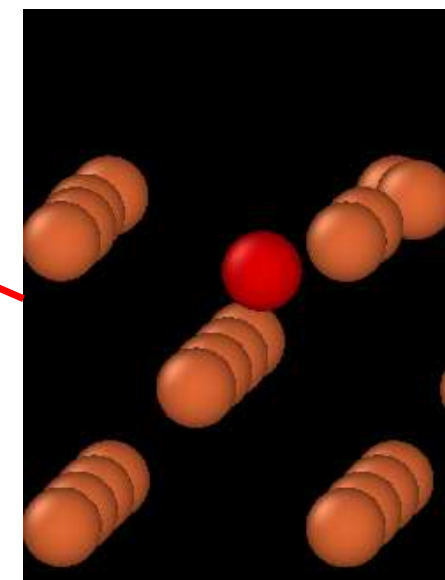
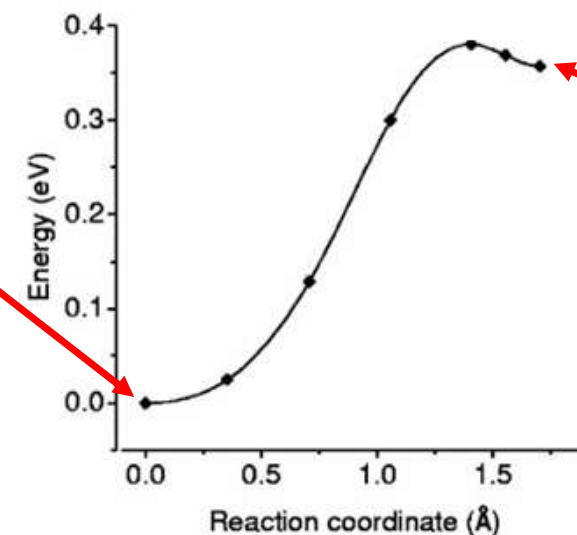
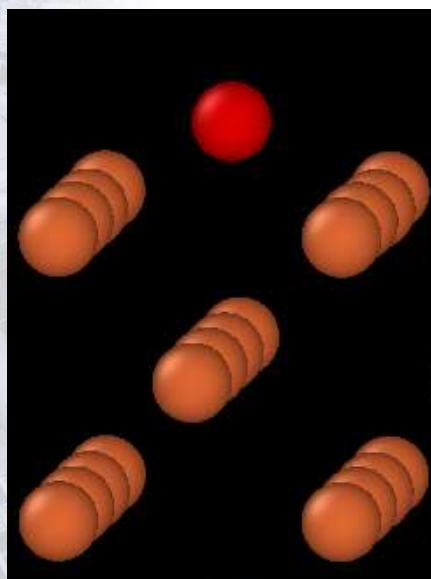


Fig13. Minimum energy path for hydrogen diffusion into Fe (100)
PHYSICAL REVIEW B 70, 064102 (2004)

4. Hydrogen solubility in bcc Fe

4.1. Outline (2/4)

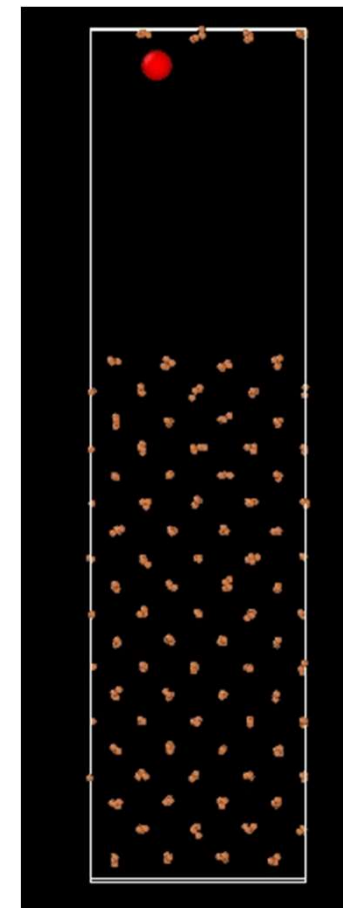
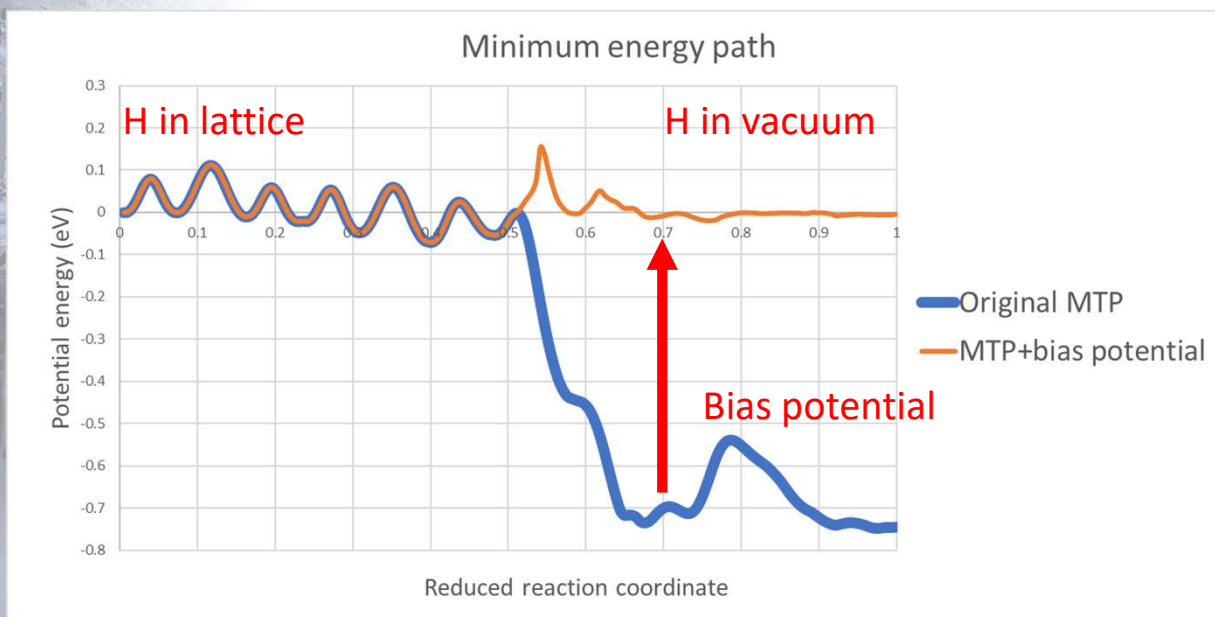


Fig14. Accelerated MD simulation for solubility estimation in bcc Fe

4. Hydrogen solubility in bcc Fe

4.1. Outline (3/4)

- ✓ The equilibrium concentration is determined so that the chemical potential of H is the same between gas state and solute state.

$$(Eq. 1) \quad \mu_{\text{solute}}(T, c_H) = \mu_{H\text{-in-}H_2\text{-gas}}(T, p_{H_2}, E_{s-H_2}) = 0.5\mu_{H_2\text{-gas}}(T, p_{H_2}, E_{s-H_2})$$

- ✓ In the present MD simulation, the equilibrium concentration with **ideal H monoatomic gas** is obtained by MD.

$$(Eq. 2) \quad \mu_{\text{solute}}(T, c_H) = \mu_{\text{ideal-}H\text{-gas}}(T, p_{\text{ideal-}H}, E_{s-\text{ideal-}H})$$

- ✓ Finally, to obtain the relation (=solubility constant) of Eq. 1 between p_{H_2} and c_H at a given temperature, we calculate the relation for H₂ gas and ideal H gas by means of **statistical thermodynamics**.

$$(Eq. 3) \quad \mu_{\text{ideal-}H\text{-gas}}(T, p_{\text{ideal-}H}, E_{s-\text{ideal-}H}) = 0.5\mu_{H_2\text{-gas}}(T, p_{H_2}, E_{s-H_2})$$

- ✓ Here, one remaining challenge is that the DFT calculation for H₂ gas is not sufficiently accurate. Thus, we use ab-initio full configuration interaction (FCI) calculation for H₂ gas thermodynamics, and E_s was optimized to best reproduce the experimental data.

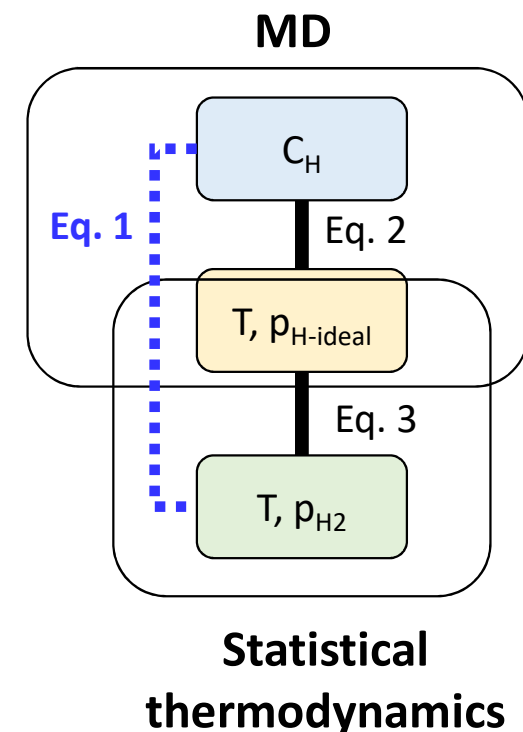
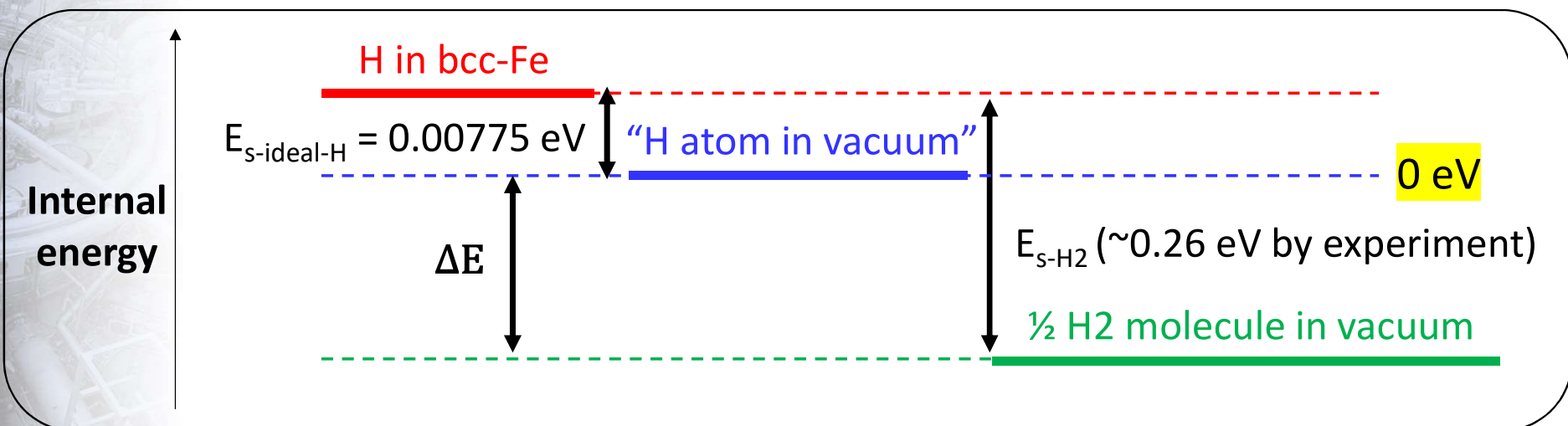


Fig16. Schematic view for solubility estimation

4. Hydrogen solubility in bcc Fe

4.1. Outline (4/4)

<Step-2: Statistical dynamics for converting $p_{\text{ideal-H}}$ to p_{H_2} >



The chemical potential of “H atom in vacuum” is obtained from the Sackur-Tetrode eqn.

$$\mu_{\text{ideal-H-gas}}(n, p, T) = \left(\frac{\partial G}{\partial n} \right) = \frac{G_{\text{ideal-H-gas}}}{n} = RT \left\{ -\frac{5}{2} \ln(k_b T) - \frac{3}{2} \ln\left(\frac{2\pi m}{h^2}\right) + \ln p_{\text{ideal-H}} \right\}$$

$$\begin{aligned} & \mu_{\text{ideal-H-gas}}(T, p_{\text{ideal-H}}, E_{s-\text{ideal-H}} = 0) \\ &= 0.5 \mu_{\text{H}_2\text{-gas}}(T, p_{\text{H}_2}, E_{s-\text{H}_2} = \Delta E) \sim -61212 + \frac{1}{2} RT \ln\left(\frac{p_{\text{H}_2}}{1 \times 10^5}\right) - \Delta E \quad \text{for } p_{\text{H}_2} < 1 \times 10^8 \text{ Pa} \end{aligned}$$

4. Hydrogen solubility in bcc Fe

4.2. Results (1/3)

<Step-1: Classical MD calculations using the biased potential>

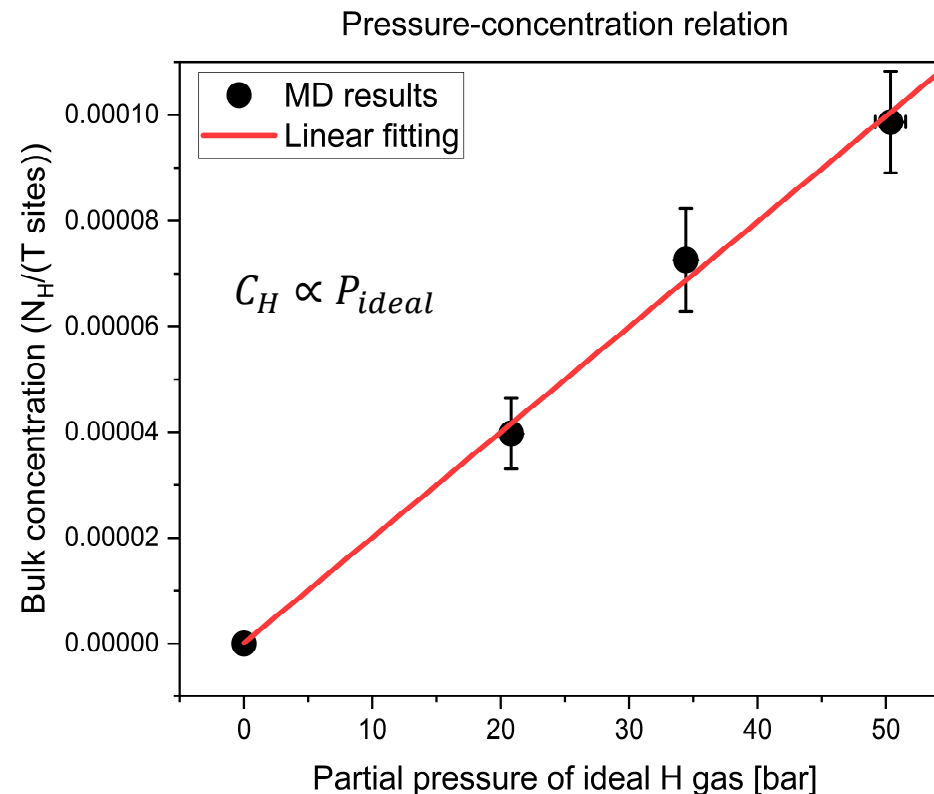
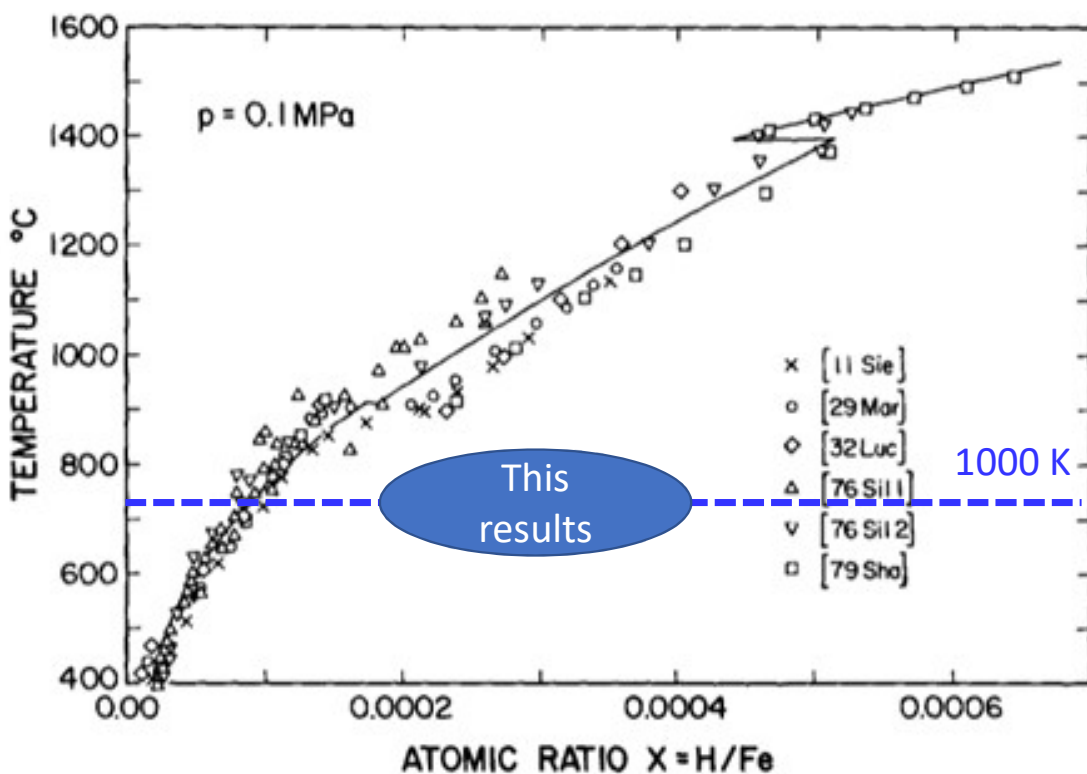


Fig15. Pressure-concentration relation in bcc Fe

4. Hydrogen solubility in bcc Fe

4.2. Results (2/3)

- ✓ Comparison with experimental data at 1000 K indicates $\Delta E = 0.37$ eV.
 - ✓ This value is reasonably close to the solution enthalpy calculated by DFT, $\Delta E = 0.29$ eV.



Solution enthalpy (eV)	Concentration (H/Fe)	Note
0.26	3.05e-4	Arrhenius plot of exp.
0.29	2.16e-4	DFT
0.37	2.42e-4	Fit to 1000 K exp. Data
Experiment	8.80e-5	

Table 2. Estimated concentration at 1000 K

Fig16. Experimental data of temperature-solubility relation in bcc Fe

*A. San-Martin, F.D. Manchester, Bulletin of Alloy Phase Diagrams 11 (1990) 173.

4. Hydrogen solubility in bcc Fe

4.2. Results (3/3)

- ✓ The Sievert's constant can be related to the solution enthalpy and **entropy** as follows*:

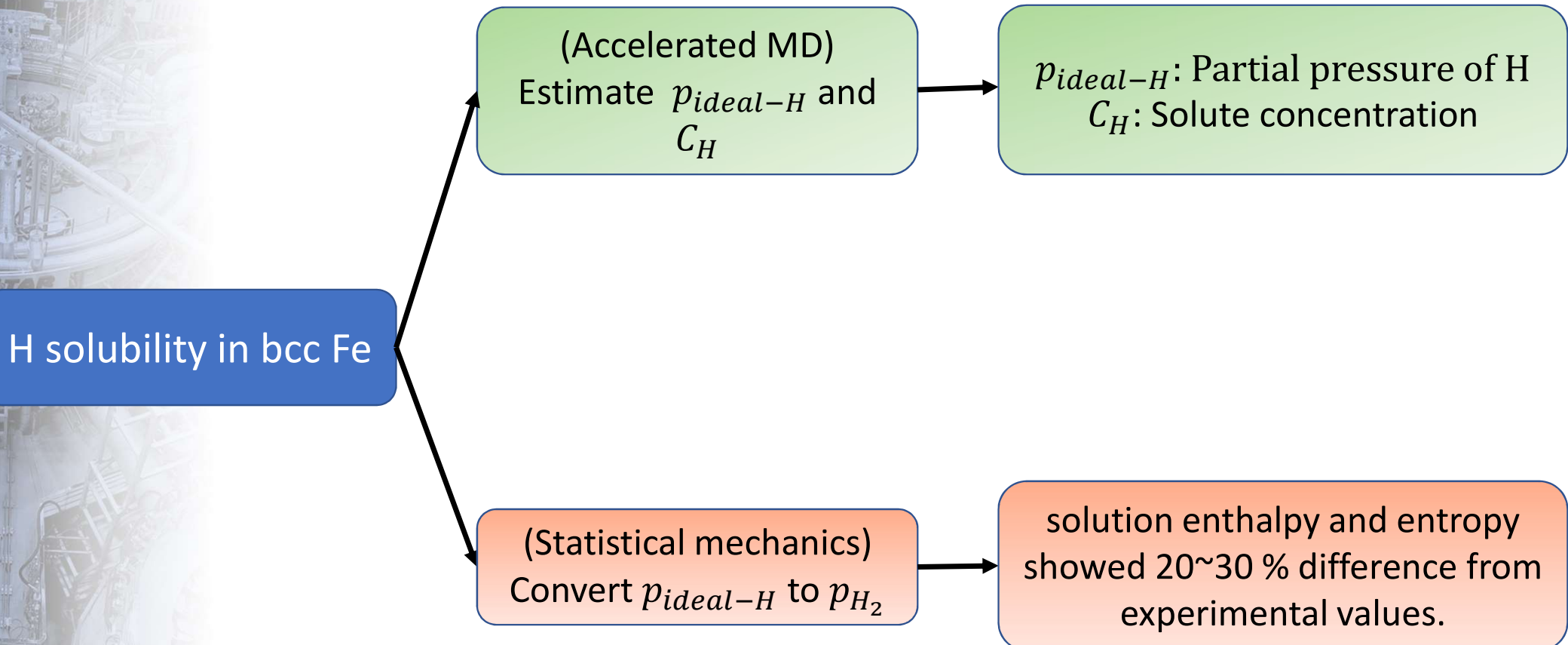
$$x = 6 \sqrt{\frac{p}{p_0}} \exp\left(-\frac{\Delta H - T\Delta S}{RT}\right)$$

Here, '6' stands for the ratio of the number of T-sites to the number of Fe atoms in bcc-lattice.

- ✓ Using the DFT data ($\Delta E = 0.29$ eV) as ΔH , the solution entropy ΔS is obtained as **-6.9R** (J/K/mol).
 - ✓ This value is close to an experimental value, **-6R***.
- ✓ Future work for improvement
 - Use equilibrium lattice constant, not geometry-optimized one.

*Y. Fukai, "The Metal-Hydrogen System", Springer (2004).

4. Conclusion



Presenter: Hyukjoon Kwon

- bagho27@snu.ac.kr

- Department of energy systems engineering, Seoul National University

Supervisor: Takuji Oda